RESONANCE IDENTIFICATION FOR IMPELLERS

by
Murari P. Singh
Chief Engineer and Manager of Engineering Technology
Bhabesh K. Thakur
Senior Structural Analyst
William E. Sullivan
Senior Structural Analyst
and
George Donald
Business Manager
GE Oil & Gas CONMEC
Bethlehem, Pennsylvania

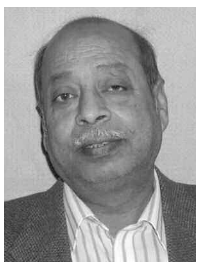

Murari P. Singh is Chief Engineer and Manager of Engineering Technology for GE Oil & Gas CONMEC, in Bethlehem, Pennsylvania. He has been involved in the design, development, and analysis of industrial turbomachinery for more than 30 years at Turbodyne Corporation, Dresser Industries, Dresser Rand, and CONMEC. Particularly, he has been involved with blade vibration, fatigue and fracture mechanics, stress and vibration of structure, reliability, life analysis, probabilistic analysis, FCC expanders, steam turbines, and centrifugal compressors.

Dr. Singh holds B.S., M.S., and Ph.D. degrees. He has authored more than 30 technical papers on a variety of topics related to turbomachinery.

Bhabesh K. Thakur, is a Senior Structural Analyst at GE Oil & Gas CONMEC, in Bethlehem, Pennsylvania. He has more than 25 years of industrial experience that includes design, fabrication, testing, research and development, structural analysis, and project management. He is currently responsible for analysis, evaluation, and validation of turbomachinery component design.

Dr. Thakur received his BSME degree (1969) from the Regional Institute of Technology, in Jamshedpur, India, MSME degree (1981) from Rochester Institute of Tech-nology, and Doctorate degree (1986) from Rensselaer Polytechnic Institute.

William E. Sullivan is a Senior Structural Analyst with GE Oil & Gas CONMEC, in Bethlehem, Pennsylvania. His primary responsibilities include stress and vibration analysis of impellers, rotor blades, and bladed disk assemblies. Other duties include general structural analyses associated with rotating machinery and related hardware. Before joining CONMEC in 1992, he was a Senior Engineer in the structures and dynamics group at Pratt & Whitney Aircraft, in East Hartford, Connecticut, where he worked mostly on fan blade flutter testing and rotordynamics. Other experience includes various technical positions with the Combustion Turbine and Large Steam Turbine divisions of the Westinghouse Electric Corporation.

Mr. Sullivan has a B.S. degree (Engineering, 1977) from Widener University, in Chester, Pennsylvania, and is a registered Professional Engineer in the State of Connecticut.

ABSTRACT

The reliability of centrifugal compressors for the most part depends on the reliable operation of impellers. Most of the time, damage to impellers is due to mechanical fatigue. Fatigue damage has been observed in blades, discs, and covers. The damage is due to alternating stress resulting from vibration of structure. Alternating force can excite natural mode(s) of vibration that in turn may result in high alternating stresses.

Analysis of a blade by itself, or for that matter a disc or cover by themselves, is easier. However, in reality, the impeller is a system that combines the blade, disc, and cover (impeller with shroud). The dynamic behavior of such a system becomes complex compared to that just for blades or just a disc. Understanding the dynamic behavior is important to rationalize fatigue failures and thus design a reliable impeller.

This paper presents:

- The results of the finite element analysis (FEA) of a simple impeller. These results help in the understanding of the behavior without the complexity of the results, thus paving the way to understand the behavior of similar complex systems. Specifically, it helps to:
    - Rationalize the results of the system based on the results of blade alone and of disc alone.
    - Describe a method to create an interference type diagram.
    - Explain the results based on the diagram.
- The results of the FE analysis for an impeller, and
- A method that helps in drawing conclusion(s) about the possible resonance of an impeller.

INTRODUCTION

The impeller of a centrifugal compressor is a circular symmetric structure. The required number of blades is machined on a circular disc. Depending on the design, there also might be a circular cover at the tip of the blades. When there is no cover, the impeller is called an open impeller.

Fatigue of metal has been observed to cause damage to impellers most of the time. Fatigue damage has been observed in blades, discs, and covers. It is known that alternating stresses induced by the vibration of structure can cause fatigue damage in impellers. Forces that vary with time can excite natural mode(s) of vibration. Excitation of a natural mode induces alternating stresses in the structure. Nelson (1979) stated that one possible cause of high alternating stresses is the resonant vibration of a principal mode. He mentioned that the vibratory mode most frequently encountered is of the plate type involving either the cover or the disc. Nelson described a fatigue failure pattern that originates at the outside diameter of the impeller adjacent to blades and fatigue crack and propagates along nodal lines on the disc or the cover. Finally, a thumbnail shaped material tears out.

Wang, et el. (1999), also argued that understanding the natural modes of vibration is essential in solving failures of open impellers. She pointed out that fatigue failure had been observed in blades of open impellers as well as in the disc.

The modes responsible for the fatigue cracks described by Nelson (1979) are those that exhibit primarily axial motion of the disc and the cover. Another type of failure experienced in an impeller is where fatigue cracks follow “a thumb nail” or “scallop” shape in blades. Figures 1 and 2 show pictures of such a failure in an impeller having fatigue cracks in blades. Fatigue cracks of this type in blades are the characteristic of modes in which blade motion is predominant. Typically, motion of the structure in the modes associated with this type of failure is in the tangential direction.

Figure 1. Photograph Showing Thumb Nail or Scallop Fatigue Cracks in Impeller.

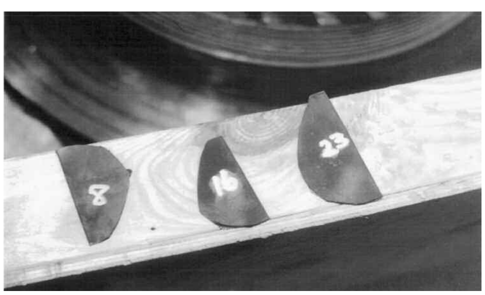

Figure 2. Photograph Showing Separated Scalloped Material.

An impeller consisting of blades, disc, and cover is one system. The structure vibrates as a whole. In some modes of vibration, the blades might be moving more than the cover or the disc. On the other hand, the cover might move appreciably more than the blades in some modes. Analysis of a blade by itself, or for that matter a disc or cover by themselves, is easier. However, in reality, the impeller is a system that combines the blade, disc, and cover (impeller with shroud). The dynamic behavior of such a system becomes complex compared to that just for blades or just a disc. Understanding the dynamic behavior is important to rationalize fatigue failures and thus design a reliable impeller.

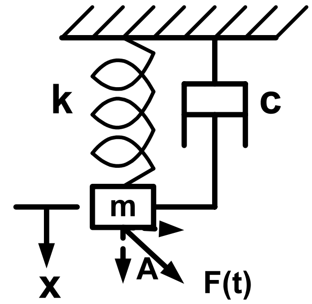

$$m.a + c.v + k.x = F(t).\cos(A)$$

Figure 3. Single Spring-Mass-Damper System.

Theoretical and experimental data were presented in the earlier work of Ewins (1970, 1973). The work explained the bladed disc behavior relating to resonance of bladed disc.

Singh, et al. (1982, 1988, 1989), presented the concept of an interference diagram for packeted bladed disc for steam turbine. Bloch (1996) described the same method of the interference diagram to evaluate the vibrational characteristics of steam turbine discs. The method has been successfully applied in the design of turbine discs ever since. The method is equally applicable to any axisymmetric structure of turbomachinery, particularly when the fluctuating forces are a function of rotational speed of the machine.

The logic and justification for extension of the concept of an interference diagram for impellers are provided in this paper. The modes of vibration of a closed impeller are similar to those of a continuously banded (shrouded) bladed disc as used in steam and gas turbines. However, the interpretation of modal results can be confounded by the complex coupling between the cover and disc caused by the twisted blade of many impellers.

Analysis of a simple similar structure is helpful to understand the behavior and then relate it to a complex structure such as an impeller. Researchers, namely Muszynska and Jones (1981) and Jones and Muszynska (1983), have utilized simple spring-mass models to understand the complex effects of couplings found in real mechanical structures. Finite element analysis has been used for a simple structure. The impeller examined is of a “2-D” (two-dimensional) blade design. This means that the blades extend straight out from the disc to the cover.

A discussion of the condition of resonance, analysis of a blade, a disc, an open impeller, and an impeller with cover will be provided. Results of an FEA are used to draw an interference diagram for impeller (IDI). Further discussion is provided for the assessment of the reliability of an impeller based on these results.

Finally, FEA results to understand the damage in blades of an impeller are presented along with the FEA results of the successful modification. The results are discussed in the light of the concept of IDI to explain and possibly understand the cause of damage and success of the modified structure.

BRIEF REVIEW OF THEORY

A detailed analysis of vibrational characteristics of a mechanical structure can be found in any textbook on mechanical vibration. The intent of this section is to highlight some concepts that will be useful later in the interpretation of the vibration of impellers. A mechanical structure such as an impeller has infinite degrees of freedom (DOF). The number of natural modes of vibration of a mechanical structure equals the number of DOF. Use of the concept of generalized coordinates facilitates the solution of a multidegree of freedom system. This method decouples each mode of vibration. Each isolated natural mode by itself of such a structure (in a generalized coordinate system) can be considered as a single spring-mass system. Therefore, the study of the dynamics of a single spring-mass-damper system will be helpful in understanding the behavior of a complex system, e.g., an impeller.

Let us consider the single spring-mass-damper system acted upon by a variable force as shown in Figure 3. Newton's third law of motion states that every action has equal and opposite reaction. The equation of motion for the above case is written as:

$$m\,a + c\,v + k\,x = F(t).\cos(A) \tag{1}$$

where:
m = Mass
a = Acceleration of the mass, *m*
c = Viscous damping
v = Velocity of the mass
k = Stiffness
x = Vertical displacement

$F(t) = F_0 \sin(\omega t)$ is the time dependent force, and the angle, *A*, defines the direction of force from the vertical direction.

Let us assume a solution for the displacement, *x(t)*, to be:

$$x(t) = A_0 \sin(\omega t + \phi) \tag{2}$$

where A_0 is the amplitude of vibration of the mass in the vertical direction when the force, *F(t)*, is applied to the mass, *m*. On the other hand the displacement of the mass, *m*, will be equal to F_0/k when a constant force equal to F_0 is applied. F_0 is the amplitude of the force. The ratio of the two displacements (the displacement due to a force that varies with time to the displacement of a constant force is having the same magnitude) is called the magnifier.

Absolute magnitude of the magnifier is given by the following expression:

$$Abs(A_0 k / F_0) = \cos(A) / \left(\left(1 - r^2\right)^2 + (2\zeta r)^2 \right)^{1/2} \tag{3}$$

where:
$r = \omega/\omega_n$
$\omega_n = (k/m)^{1/2}$
$\zeta = c/(2(km)^{1/2})$
A_0 = Amplitude of vibration
F_0/k = Displacement if the magnitude of an applied steady-state force is equal to F_0

The magnifier as a function of the frequency ratio, *r*, for different damping is plotted in Figure 4. Each curve shows that the magnifier attains highest magnitude when *r* is near unity.

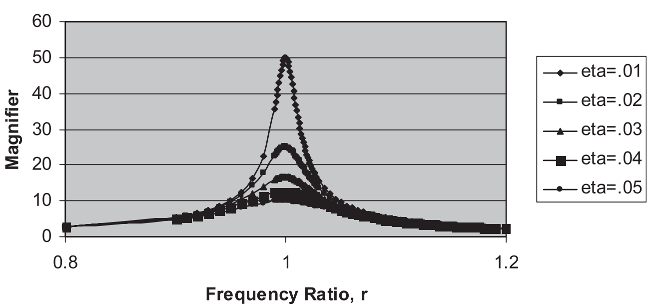

Figure 4. Absolute Value of Magnifier Versus Frequency Ratio.

The other interesting result is obtained by plotting the inverse of the magnifier as a function of the frequency ratio, *r*, as shown in Figure 5. The inverse of the magnifier is the resistance of the mechanical structure to the alternating force. The resistance attains its minimum value when the frequency ratio is equal to one.

Figure 6 shows variation of peak response of the mass as a function of the direction of the force. The degrees of freedom of

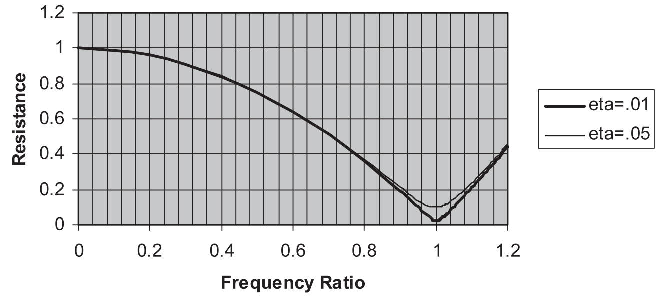

Figure 5. Resistance Versus Frequency Ratio.

the spring-mass-damper (SMD) system is the displacement in the vertical direction, i.e., the mass can move only up and down. The system will respond only to the vertical component of the force, *F*. The response is the largest when the force acts in the vertical direction (angle, *A*, equal to zero), and the response is zero when the vertical component of the force is zero (angle, *A*, equal to 90 degrees). The mode shape (motion pattern in the vertical direction) matches only with the vertical component of the force. When the acting force is in the horizontal direction, its shape does not match with the up and down motion of the mass, resulting in zero response.

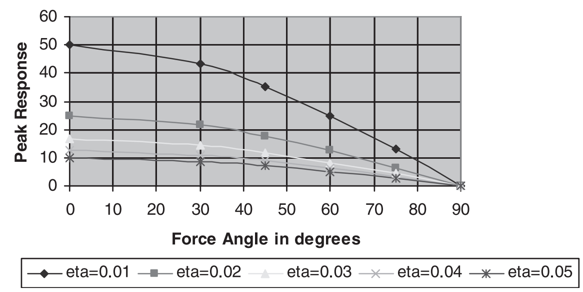

Figure 6. Peak Response Versus Angle of Force.

Discussion of Resonance

Singh, et al. (1988), discussed resonance of circular symmetric structure and pointed out that resonance can be viewed to be a state when energy built up in the system due to applied forces attains a maximum value. Thus, in the state of resonance, the magnitude of response (stress, displacement) of the system also attains its maximum value and the system's resistance to the exciting forces is minimum (Figure 4 and Figure 5).

The following two conditions were also mentioned for a mechanical structure to be in a state of resonance: frequency of the exciting force equals the natural frequency of vibration, and the profile (shape) of the applied force should have the same shape as the mode shape associated with that natural frequency.

Mathematical expressions were also provided to support that each one of the above conditions is necessary for resonance to occur but not sufficient in itself. For resonance to occur both conditions must be satisfied at the same time. The time varying periodic forces experienced by rotating blades can be resolved in harmonics. Resolution of harmonics is accomplished by performing Fourier decomposition of the periodic force shape. The frequencies of the harmonics are integer multiple of the speed of rotation. In general, the force experienced by the blades of an impeller during a complete revolution is the consequence of any circumferential distortion in the flow, etc.

The frequency of the excitation due to inlet guide vanes or due to diffuser vanes is given by:

$$k.\omega = (K.N)/60 \tag{4}$$

where:
$k.\omega$ = Frequency, Hz

K = Number of distortions in flow per 360 degrees, e.g., number of IGV, or number of vanes, in the diffuser, etc.
N = Compressor's speed, rpm

K also represents the shape of the excitation as *k* nodal diameter. K_{th} harmonic of the force felt by blades can be written as:

$$P_k(\theta,t) = P_k \, Sin \; k(\omega t + \theta) \tag{5}$$

where the frequency of the force is $k\omega$ and θ is the angle on the disc from a reference point. The mode shape with m nodal diameters and with the natural frequency, ω_m, can be expressed as:

$$X_{\underline{m}}(\theta,t) = -A_m \, Cos\left(\omega_m t + m\theta\right) \tag{6}$$

The condition of resonance can occur when the alternating force does positive work on the blade.

Work done is a function of displacement and it is expressed as dW = P(x).dx. A graphical depiction of work done by a force, *P*, is shown in Figure 7.

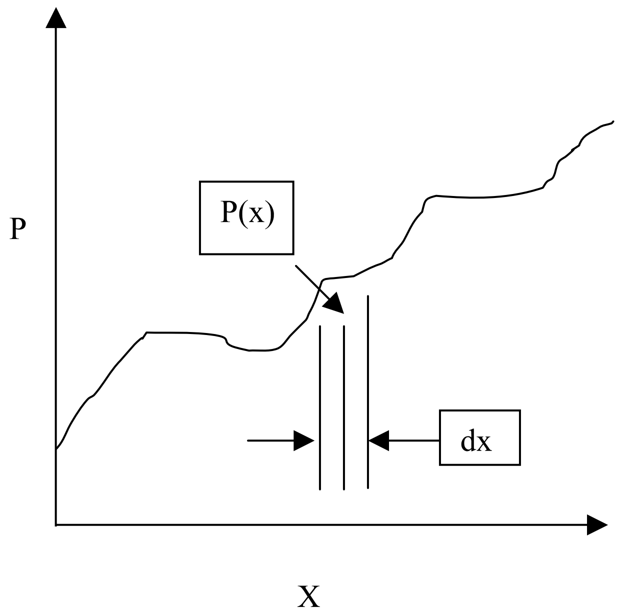

Figure 7. Graphical Depiction of Work Done by Force, P.

The work done by the k_{th} harmonic of the force acting on mode shape having *m* nodal diameters in one complete period (*T*) can be expressed as follows:

$$W = \int_0^{2\pi}\int_0^{T} P_k(\theta,t)\frac{d}{dt}X_m(\theta,t)\frac{N}{2\pi}dt\, d\theta$$

$$= \int_0^{2\pi}\int_0^{T} P_k \, Sin\, k(\omega t + \theta)\omega_m A_m Sin(\omega_m t + m\theta)\frac{N}{2\pi}dt\, d\theta \tag{7}$$

$$= \begin{cases} N\pi P_k \; A_m & (for\ m = k\ and\ \omega_m = k\omega) \\ 0 & (for\ m \neq k\ or\ \omega_m \neq k\omega) \end{cases} \tag{8}$$

The first expression of Equation (8) is the positive work ($N\pi P_k A_m$) done by the force. The first expression is true only if the nodal diameter (*m*) of the mode shape is the same as the shape of the k_{th} harmonic of the force, and the natural frequency (ω_m) of vibration is equal to the frequency ($k\omega$) of the force.

The zero work results when either the nodal diameter (*m*) of the mode shape is not the same as the shape of the k_{th} harmonic of the force, or the natural frequency (ω_m) of vibration is not equal to the frequency ($k\omega$) of the force.

The above argument is the basis of the interference diagram and it further explains the need for examining the frequency of vibration along with the mode shape and the shape of the force while considering resonance.

FE ANALYSIS AND RESULTS

In general, the impeller rotor assembly has a complex geometry. The blades are designed to be aerodynamically efficient to provide minimum frictional energy loss. To achieve this condition, the blade is formed in 3-D (three-dimensional formed shape) and welded to the disc and cover. The simpler designs have 2-D formed blades that can be machined as an integral part with the disc. The cover is then welded to the blades. Final machining produces the designed dimensions.

A series of finite element analyses has been done, which includes a single blade, the disc alone, an open impeller, and an impeller with cover.

SINGLE BLADE

A single blade was modeled by using brick type elements. FE model of the blade has 224 elements, 405 nodes, and 1215 degrees of freedom. Two different boundary conditions were used. First, the blade was considered cantilevered on the face where the blade nodes coincide with the nodes on the disc. This analysis is done to correlate single blade mode shape with the mode shape of the open impeller. For the second analysis, the nodes on one face of the blade coincide with the nodes on the disc, and the nodes on the other face of the blade coincide with the nodes on the cover. The boundary condition of the second case was used to correlate the blade mode shapes with the mode shapes of impeller with cover.

Case 1—Single Blade with Cantilever Boundary Condition

The first case is to analyze a single blade with a cantilevered boundary condition where the blades are in contact with the disc. The FE model is shown in Figure 8 with a fixed boundary condition. The nodes of the blade that coincide with the nodes on the disc surface were constrained in all directions. The first two mode shapes of vibration are shown in Figure 9 and Figure 10. The information of interest is the displacement pattern of these modes and how it is related to the vibration modes of the open impeller.

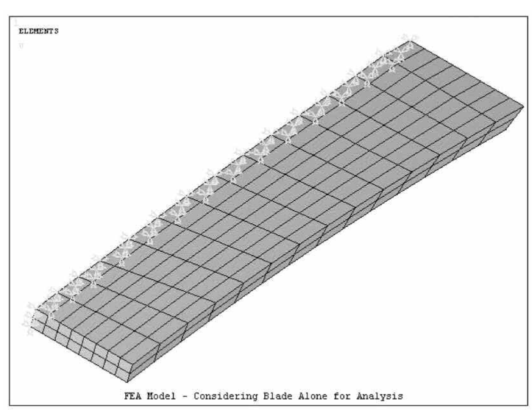

Figure 8. Finite Element Model for Single Blade.

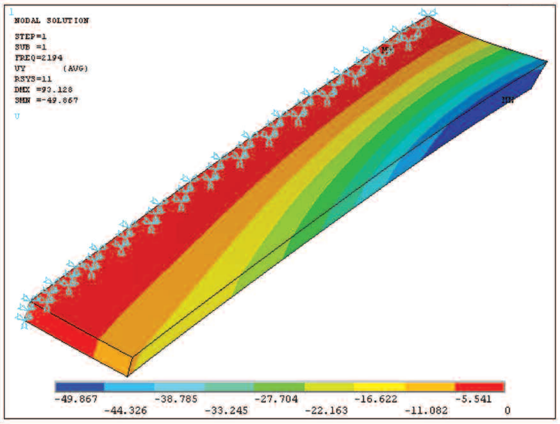

Figure 9. First Bending Mode Shape of Cantilevered Single Blade.

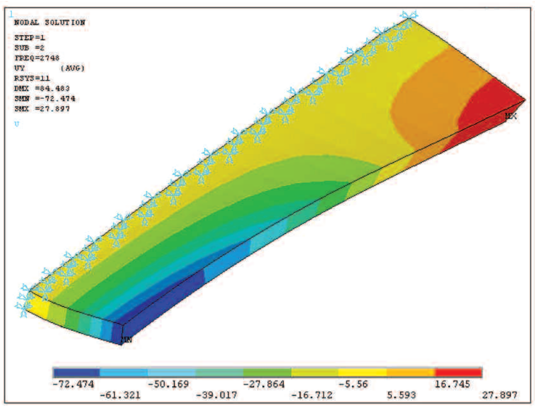

Figure 10. Second Bending Mode Shape of Cantilevered Single Blade.

Case 1B—Single Blade with Both Ends Fixed

This case is a repeat of the previous case with the face of the plate that touches the cover also being fixed. This simulates the condition when blades are thin and, on the other hand, the disc and cover are thick. Nodes that coincide with the disc and with the cover were constrained in all directions. The first three mode shapes of vibration are shown in Figures 11, 12, and 13. Again the information of interest is the displacement pattern of these modes and how these are related to the vibration modes of the impeller with a cover.

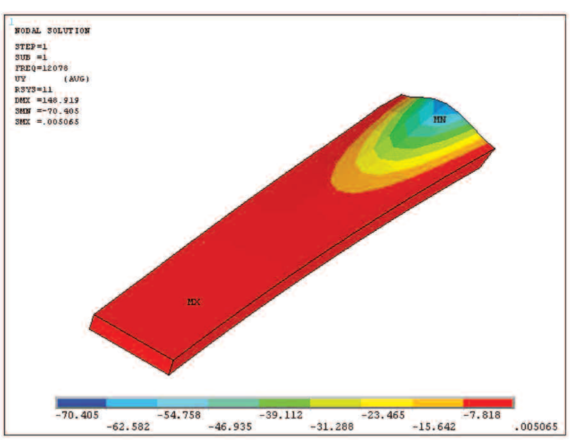

Figure 11. First Bending Mode Shape of Single Blade Fixed at Both Ends.

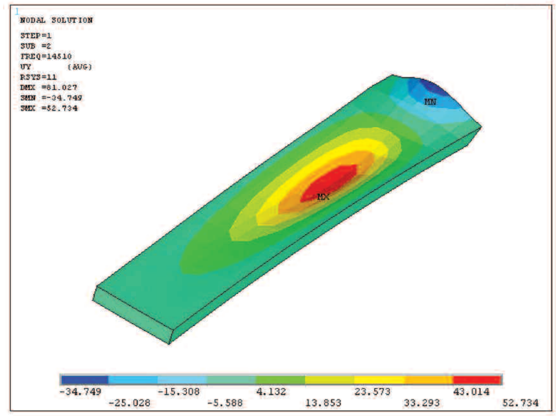

Figure 12. Second Bending Mode Shape of Single Blade Fixed at Both Ends.

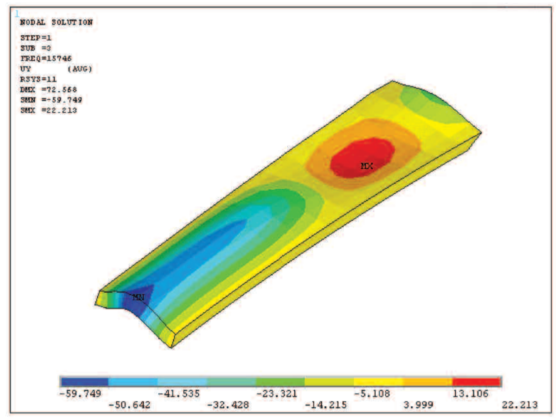

Figure 13. Third Bending Mode Shape of Single Blade Fixed at Both Ends.

DESCRIPTION FOR FEA MODEL OF IMPELLER

A proprietary procedure facilitated the FE model generation of the complex shape of the impeller. The FEA model has been created using a commercially available software 3-D brick element (eight nodes). Each node has three degrees of freedom. These are translations in the nodal x, y, and z directions. To generate elements for the blade, the finite element nodes are created at the intersection of the blades with the disc as well as with the cover. Then desired numbers of elements are created after generating nodes in between disc and cover. Depending on the number of blades, the accuracy level, computer capacity, and processing time, nodes and elements are generated for 360 degree rotation to create a complete model. The impeller that has been analyzed has 23 blades. The number of nodes, elements, and DOF for different components of the impeller for this evaluation is provided in Table 1.

Table 1. The Number of Nodes, Elements, and Degrees of Freedom for Different Models.

Component	No. of Nodes	No. of Elements	DOF
Disc alone	13,800	8832	41,400
Open impeller	23,115	13,984	70,000
Impeller with cover	32,499	19,872	97,492

The disc bore nodes are constrained fully (in all directions) in the region of the interference fit to simulate assembly condition. The blade nodes are joined with the elements of the disc and cover at the intersection using constraint equations.

Case 2—Disc Alone

The disc is another basic component of an impeller. A finite element model of the disc is given in Figure 14. A few mode shapes are also shown in Figures 15, 16, 17, and 18.

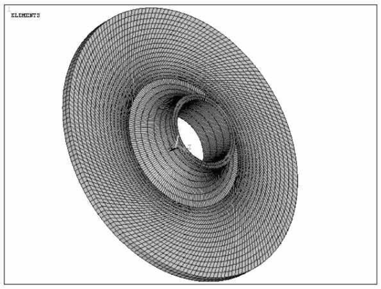

Figure 14. Finite Element Model for Disc Alone.

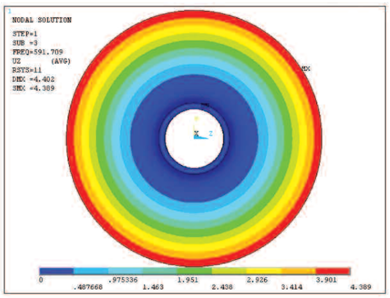

Figure 15. Umbrella (0 Circle and 0 Nodal Diameter Mode) for Disc.

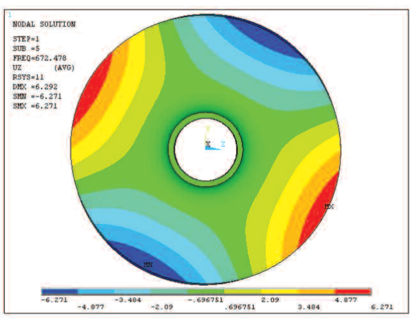

Figure 16. Zero Circle and 2 Nodal Diameter Mode for Disc.

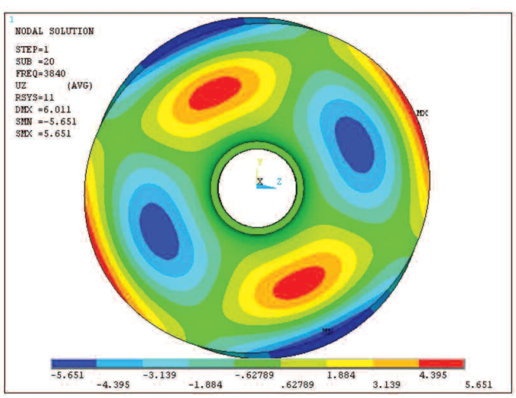

Figure 17. One Circle and 2 Nodal Diameter Mode for Disc.

Case 3—Open Impeller

An analysis was performed for an open impeller that contained the disc and 23 blades previously analyzed. The FE model is shown in Figure 19. A few mode shapes are also shown in Figures 20, 21, 22, and 23.

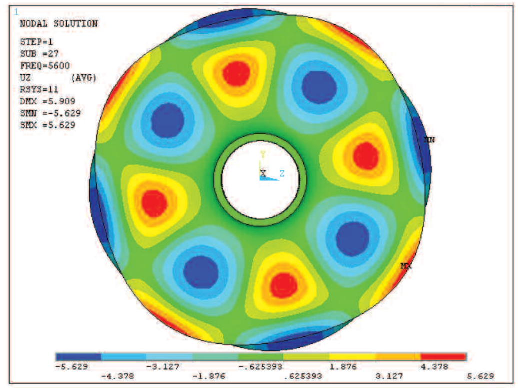

Figure 18. One Circle and 4 Nodal Diameter Mode for Disc.

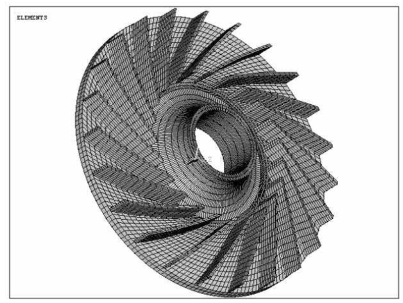

Figure 19. Finite Element Model of Open Impeller.

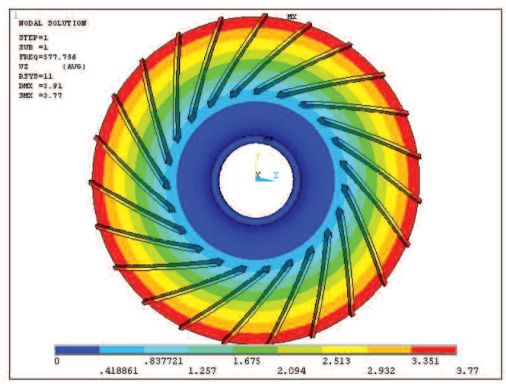

Figure 20. Umbrella (0 Circles and 0 Nodal Diameters) Mode Shape of Open Impeller, Displacement in Axial Direction.

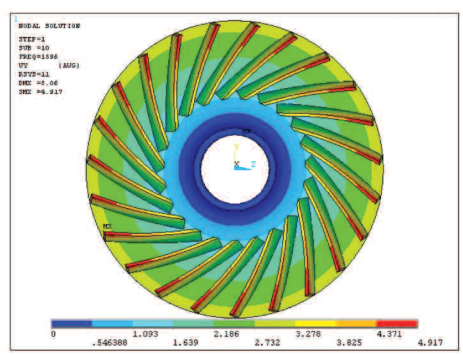

Figure 21. Umbrella (0 Circles and 0 Nodal Diameters) Mode Shape of Open Impeller, Displacement in Tangential Direction.

Case 4—Impeller with Cover

An analysis was performed for an impeller with a cover that has the same 23 blades described earlier. A FE model is shown in Figure 24. Mode shapes are also shown in Figures 25, 26, and 27.

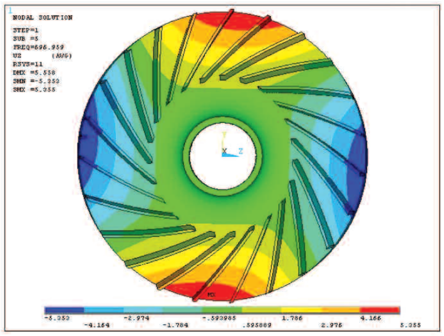

Figure 22. Zero Circles and 2 Nodal Diameters Mode Shape of Open Impeller.

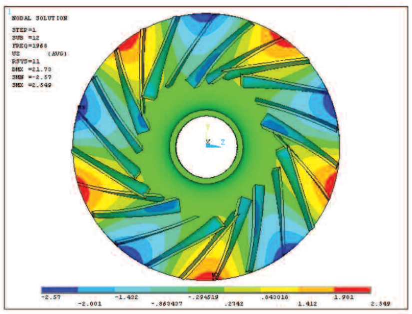

Figure 23. Zero Circles and 5 Nodal Diameters Mode Shape of Open Impeller.

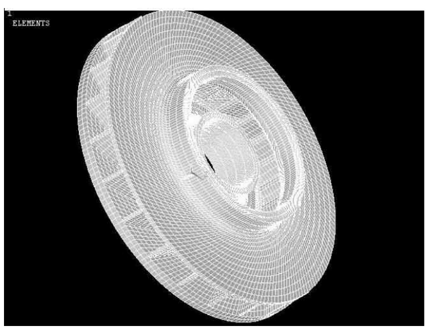

Figure 24. Finite Element Model of Impeller with Cover.

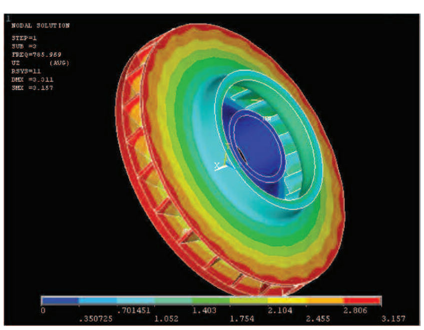

Figure 25. Umbrella (0 Circles and 0 Nodal Diameters) Mode Shape of Impeller with Cover.

FORCING FUNCTION

The most obvious sources of excitation are 1× or higher order interactions with the number of diffuser vanes, inlet guide vanes (IGV), return channel vanes (upstream or downstream of the impeller), and impeller blades.

On single stage units such as pipeline compressors, a volute tongue is a possible excitation source. Volutes (and to a greater

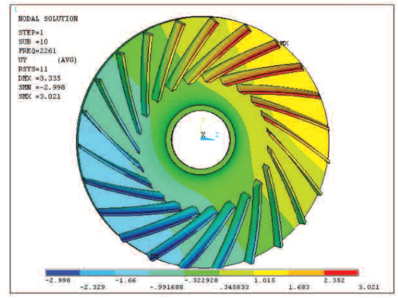

Figure 26. Zero Circles and 1 Nodal Diameter Mode Shape of Impeller with Cover, Tangential Displacement.

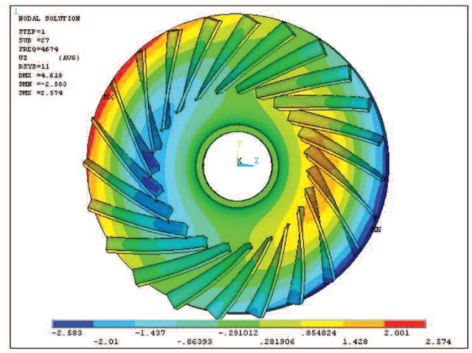

Figure 27. One Circle and 1 Nodal Diameter Mode Shape of Impeller with Cover, Axial Displacement.

extent collectors) create nonuniform pressure fields at the discharge of the impeller that could act as a forcing function.

Stall is also a potential source of excitation and can occur within the impeller or the diffuser (with vane or without vane). Stall in diffusers without vanes is characterized by one or more "cells" that rotate with (although slower than) the impeller. Stall cells have been known to cause high subsynchronous vibration.

The disc/cover cavity shape (the shape of the cavity between the disc or cover and the stationary walls surrounding the impeller) has also caused acoustic resonance that resulted in impeller failure.

General expressions are provided in Equation (4) and Equation (5) for forces that result from rotation and interruptions in the flow field.

INTERFERENCE DIAGRAM FOR IMPELLER

To describe the dynamic behavior, two pieces of information are essential, namely mode shape and natural frequency. Singh and Vargo (1989) described the method of utilizing this information to create an interference diagram for a bladed disc. The interference diagram, which combines impeller natural frequencies, impeller mode shapes, excitation frequencies, and operating speeds on one graph, is an excellent guide in determining the possibility of exciting a particular mode of vibration in an impeller. In any vibration cycle, certain parts of a mechanical structure remain stationary. For a circular symmetric system, these points fall on radii (always an even number) or circles. A pair of radii (opposite each other) is considered as a diameter. Mode shapes can be characterized by specifying the number of nodal diameters (D) and nodal circles (C). The x-axis of the diagram represents nodal diameters. Frequency is plotted on the y-axis of the interference diagram. A good design would yield an interference diagram that indicates no coincidence of possible excitation force with a natural mode of the impeller. To understand the interference diagram detail regarding a particular mode shape is essential in determining the likelihood of exciting that mode to a degree where it will adversely affect reliability.

The results of the modal analysis have been used to draw an interference diagram, and some representative mode shapes for different cases are shown in many plots in earlier sections. There are areas of zero displacements, and change in the direction of displacement from one area to the next is evident. Qualitatively, if one connects the points of zero displacement, it will result in a pair of radii and/or a circle.

The result from FE analysis provided magnitude of frequency and associated mode shapes. The natural frequencies of the impeller and the mode shapes were saved. Deflections around the disc and cover were examined using a Fourier decomposition code to quickly identify the mode shapes in terms of nodal diameter. Singh, et al. (1988), provided the reason that a maximum number of nodal diameters is equal to half the number of blades when the number of blades is even. The maximum number of nodal diameters is half of one less than the number of blades when the number of blades is odd. Plots of mode shapes were also used to verify the Fourier results and to determine the number of circles present in these modes.

The results of the Fourier analyses were divided into axial and tangential directions, depending on the prominent deflection of each mode. The modes were identified by their nodal diameter "family." Description of mode shapes by nodal diameters is a key element in the construction of the interference diagram and is essential in understanding how a structure can be excited by introducing a periodic stimulus to the blades. Mode shapes in the first family will consist of each blade displaying the first bending mode of a single blade (Figure 28 and Figure 29).

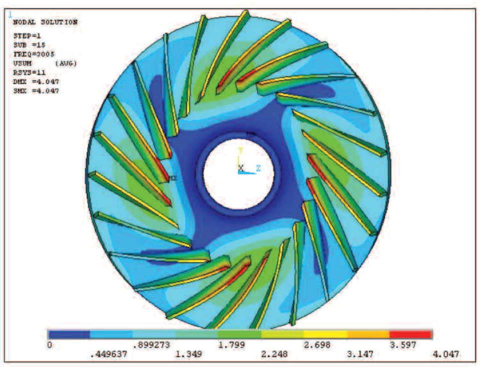

Figure 28. Mode Where Blade Shows First Mode of a Cantilevered Blade.

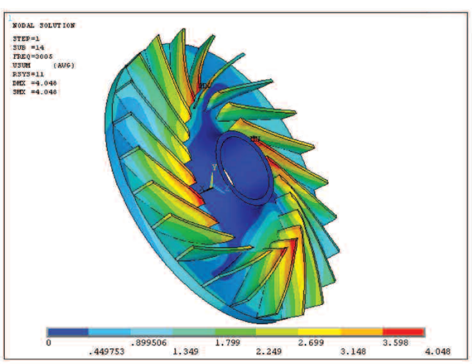

Figure 29. Another Mode Where Blade Shows First Mode of a Cantilevered Blade.

Each mode shape consists of a different number of blades moving in the same or opposite direction. For example, if half the number of blades moves in one direction, and the next half moves in the opposite direction, there is one phase change in the displacement. The pattern of displacement is similar to a single cosine or a single sine wave. Thus, it is called one nodal diameter.

Consideration of the reliability of blades of an impeller is important since in many cases blades seem to be the weakest link. The largest number of phase changes in the displacement of blades will be equal to the number of blades. Thus, the largest nodal diameter mode shape is half the number of blades in the case of an even number of blades. When the number of blades is odd the largest nodal diameter is calculated by deducting one from the number of blades before dividing in half. The number of blades is 23 in the impeller analyzed. The maximum number of nodal diameters is equal to (23 − 1)/2, or equal to 11.

Let us examine the two cosine plots of Figure 30. The subtended angle between blades is 15.65 degrees for an impeller that has 23 blades. It is clear from the plot that these two waves intersect at precisely 15.65 degrees. The implication is as follows: if each blade is instrumented to measure and thereby to determine the shape of the fluctuating force in each revolution, then both waves are equally probable. It means that a 9 nodal diameters mode of the impeller may be excited by a force that has a 14 nodal diameters shape provided frequencies are the same. There are many combinations for which this assertion is also true, but the combination is unique for each individual impeller. The combination, however, depends on the number of blades in the impeller. Another such combination for an impeller with 23 blades is 5 nodal diameters mode of the impeller may be excited by a force of 28 nodal diameters shape if frequencies are the same (Figure 31).

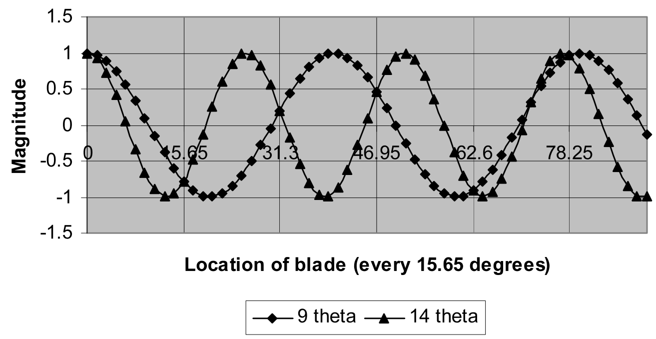

Figure 30. Cosine (9θ) and Cosine (14θ).

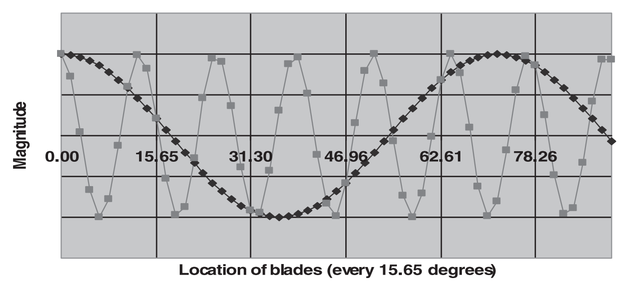

Figure 31. Cosine (5θ) and Cosine (28θ).

The previous section on resonance showed that a mode shape and the shape of the excitation should be the same for resonance. Let us consider a case where nodal diameter (the shape of the excitation) is larger than the maximum nodal diameter of the mode shape just discussed. For example, assume the number of inlet guide vanes used for the design is 14. The question is "will the force resulting from 14 IGVs excite any impeller mode that is less than 14 nodal diameters?"

The following relationships are useful in calculating possible combinations:

$$K = abs(n.L + M) \text{ and} \tag{9}$$

$$K = abs(n.L - M) \tag{10}$$

where:
n = 0, 1, 2, 3, … L

L = Total number of blades
M = Nodal diameter of mode shapes

Let us use the above relationship to generate a set of combinations for the impeller being studied having 23 blades.

Figure 32 and Figure 33 show, for example, that a 5 nodal diameters mode shape not only may be excited by a force having a 5 nodal diameters shape but also by a force of 18, 28, 41, 51, 64, 74, etc., nodal diameters shapes as long as the frequency of the force is equal to the natural frequency of the impeller. This attribute is captured in the interference diagram by the reflection of radial lines representing a constant speed.

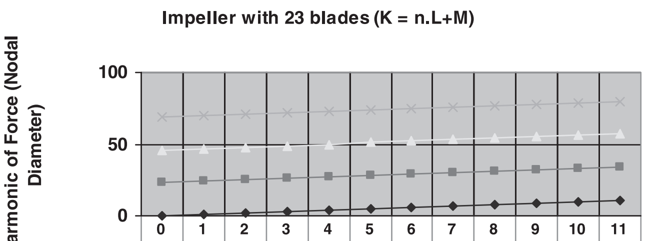

	0	1	2	3	4	5	6	7	8	9	10	11
n = 0	0	1	2	3	4	5	6	7	8	9	10	11
n = 1	23	24	25	26	27	28	29	30	31	32	33	34
n = 2	46	47	48	49	50	51	52	53	54	55	56	57
n = 3	69	70	71	72	73	74	75	76	77	78	79	80

Figure 32. Plot of Relationship Described by Equation (9).

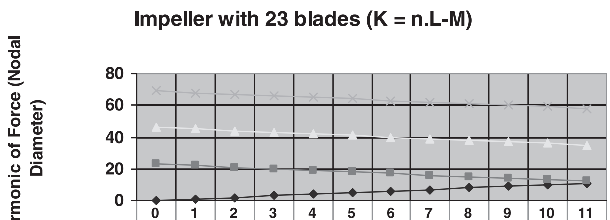

	0	1	2	3	4	5	6	7	8	9	10	11
n = 0	0	1	2	3	4	5	6	7	8	9	10	11
n = 1	23	22	21	20	19	18	17	16	15	14	13	12
n = 2	46	45	44	43	42	41	40	39	38	37	36	35
n = 3	69	68	67	66	65	64	63	62	61	60	59	58

Figure 33. Plot of Relationship Described by Equation (10).

Utilizing the concepts and methods discussed in earlier sections, the finite element analysis results for the cases studied in the form of IDI have been plotted in Figures 34, 35, 36, 37, and 38.

CASE STUDY

Concept of the interference diagram for impellers has helped in the design of reliable impellers. Also, IDI has helped to understand fatigue failures and thus helped to formulate a solution to those failures. An impeller of a pipeline compressor showed fatigue damage in many blades after a small operation time (Figure 1, Figure 2, and Figure 39).

The shape of the separated pieces was of a "scallop" type. Based on a finite element analysis supported by a frequency test, a new impeller was designed. The solution was an impeller with modified blade geometry and a change in the number of blades of the impeller. The modified design is operating successfully in the field.

The same impeller was analyzed to create an IDI for the original design as well as the modified design to take a fresh look at the possible cause of damage and the remedy thereof. Finite element analysis has been performed on the damaged impeller geometry. A parallel analysis has also been performed on the modified impeller. Figure 40 and Figure 41 show the IDI for the original and for the modified impeller geometry. Figure 40 shows resonance with the second harmonic of the possible excitation force generated by IGV.

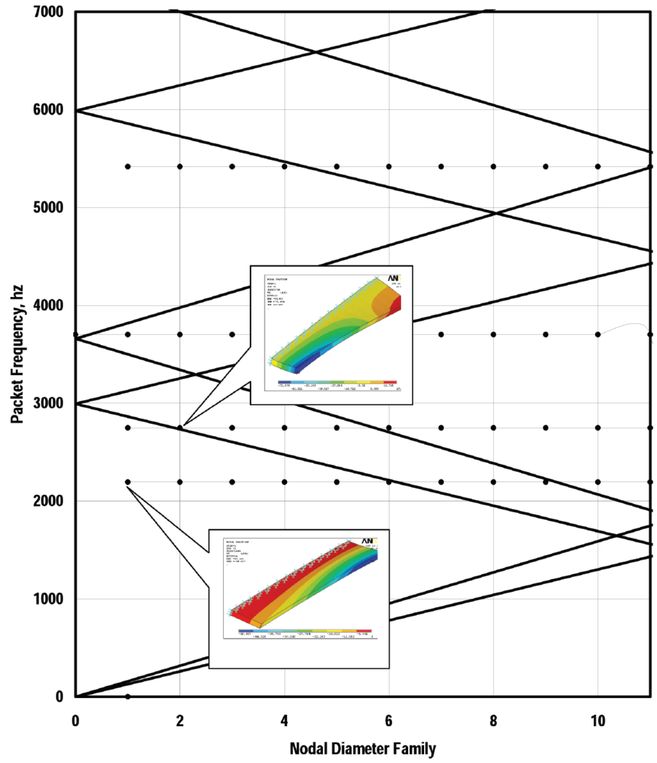

Figure 34. Interference Diagram for a Cantilevered Blade.

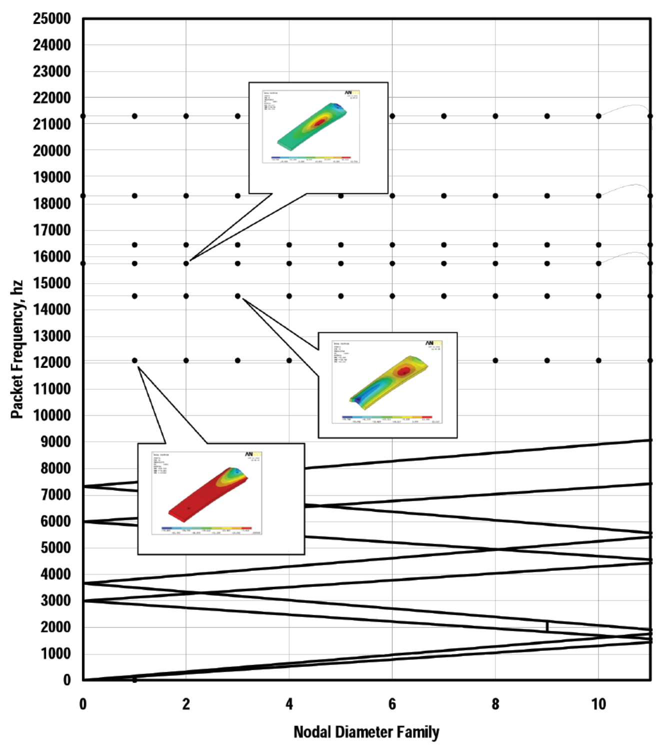

Figure 35. Interference Diagram for Blade with Both Ends Fixed.

The mode that coincides with the second harmonic of the IGV excitation is shown in Figure 42. It is instructive to note that the displacement pattern of each blade is similar to the scallop shape at the inlet where the damage occurred in the blades.

IDI also shows a possible resonant condition with a force having a shape of blade passing frequency. The force having nodal diameters equal to the number of blades can also excite a zero

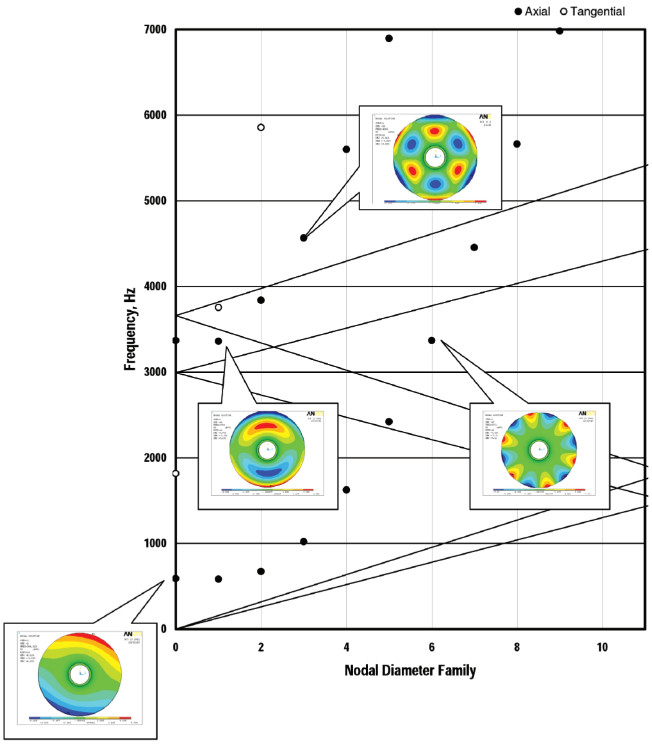

Figure 36. Interference Diagram for Disc Alone.

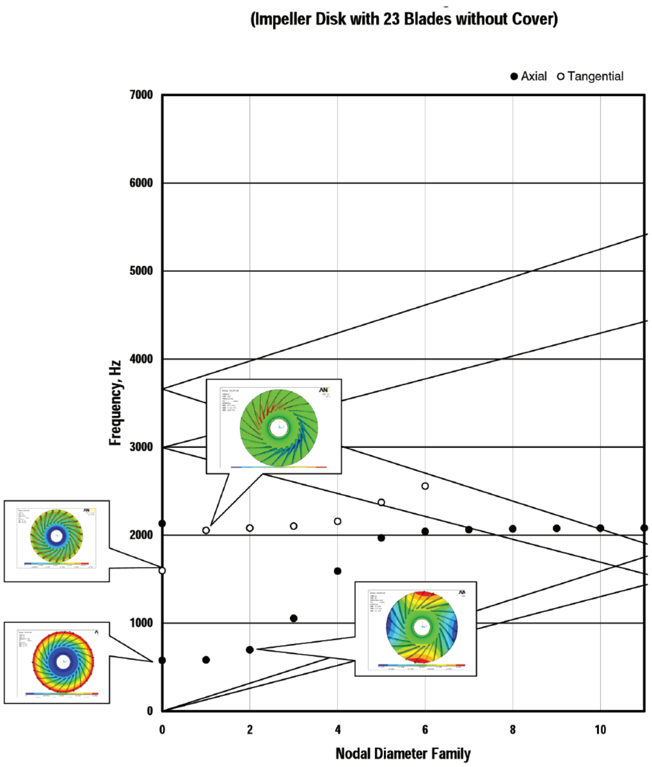

Figure 37. Interference Diagram for Open Impeller.

nodal diameter mode of vibration of the impeller if frequencies are coincident per Equation (9) and Equation (10). There are two modes that are coincident with the blade passing excitation within the speed range, shown in Figure 43 and Figure 44. In both modes of vibration the displacement pattern of each blade is also similar to the scallop shape at the inlet where the damage occurred in the blades.

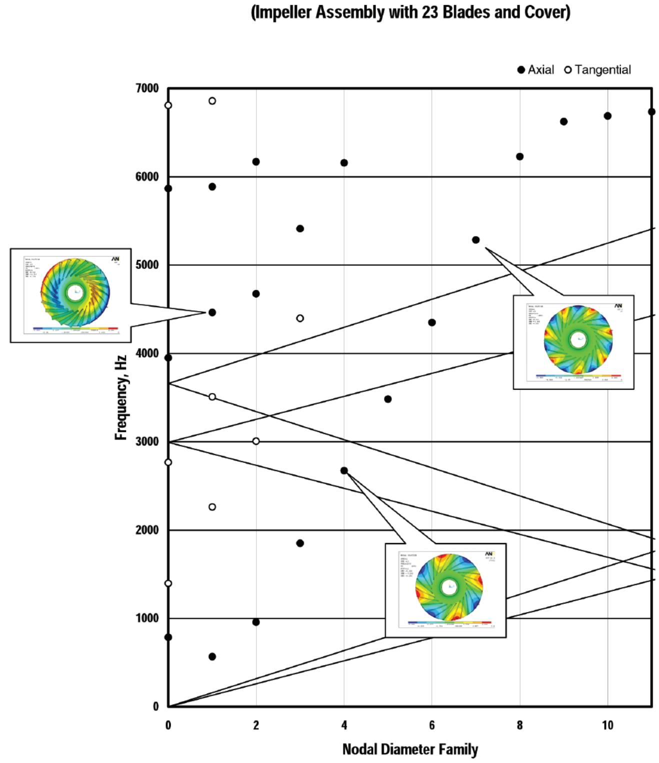

Figure 38. Interference Diagram for Impeller with Cover.

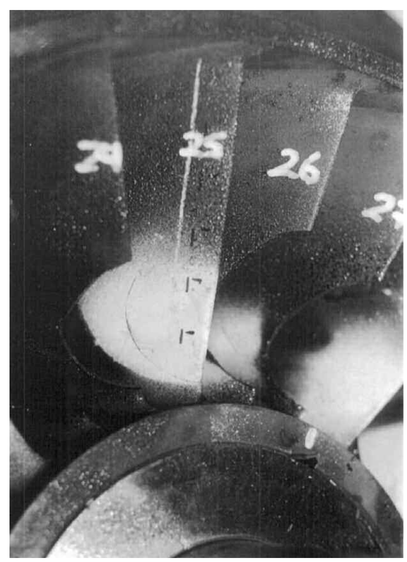

Figure 39. Scallop Shaped Break out from Blades.

For a relatively dense medium and also for a high speed application, there is a probability of a reflection of a force emanating from the rotation of blades. The impeller was modified with this in mind. The modified impeller has a different number of blades with an increased thickness. This resulted in a higher frequency for modes controlled by blades. The modified design does not have any IGV so the excitation due to vanes does not exist. The IDI (Figure 41) of this design also shows the possibility of blade passing frequency exciting a mode of zero nodal diameters. Figure 45 shows the zero nodal diameters mode of the modified design.

The original impeller failed very quickly indicating a high cycle fatigue mode of failure, but the redesigned impeller has been in operation for a long time without any distress. It can be inferred

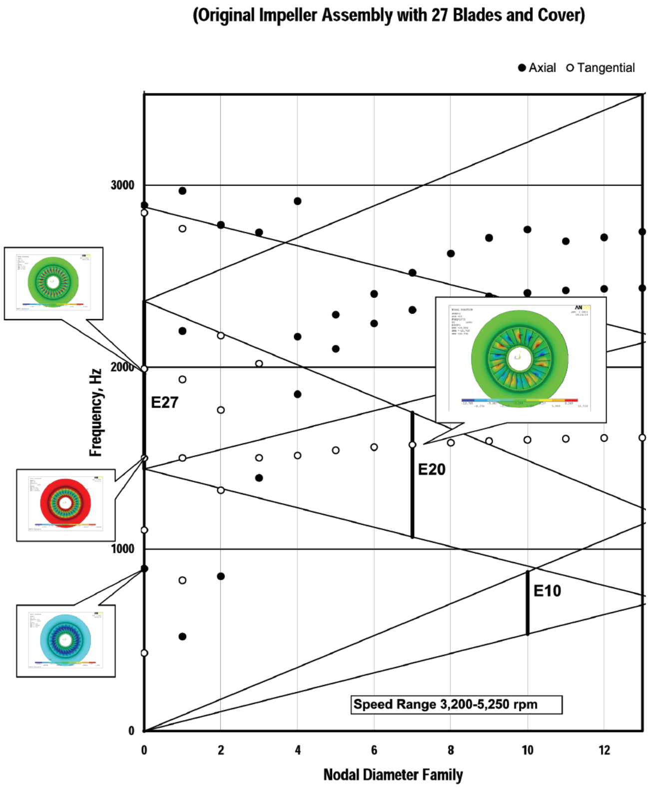

Figure 40. Interference Diagram for Original Impeller.

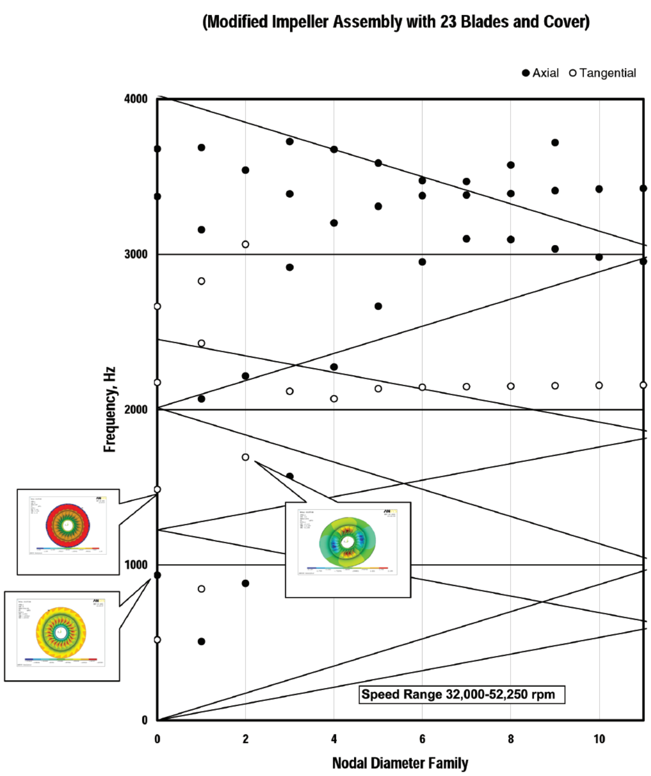

Figure 41. Interference Diagram for Modified Impeller.

from this study that second harmonics of the vane excitation might have been responsible for the damage of the original impeller. Figure 41 shows that if the reflected blade passing force was the cause of failure, then the modified design should have shown damage in operation.

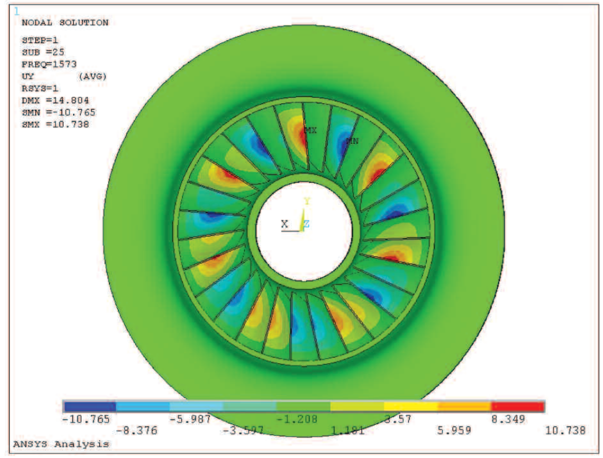

Figure 42. Seven Nodal Diameters Mode with Scallop Shaped Displacement Pattern for Blades.

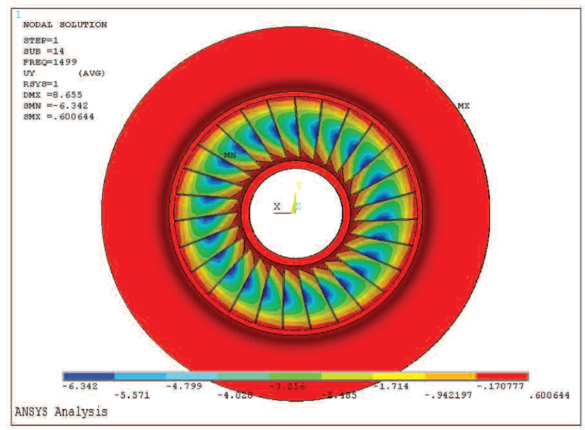

Figure 43. Zero Nodal Diameters Mode with Scallop Shaped Displacement Pattern for Blades (A).

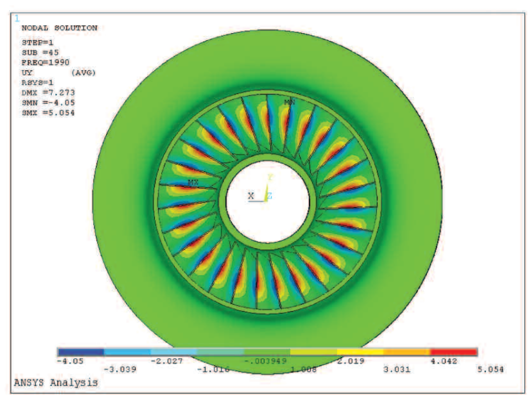

Figure 44. Zero Nodal Diameters Mode with Scallop Shaped Displacement Pattern for Blades (B).

SUMMARY

The vibration characteristics of an impeller, open or with a cover, are complex. Analytical results of finite elements helped to understand the natural mode shapes of vibration of an impeller. Interference diagrams of an impeller had been drawn for blade, disc, and impeller. Frequency is shown on the vertical axis and mode shape as nodal diameters on the horizontal axis. The IDIs applicability is demonstrated by the explanation of a successful modification of an impeller.

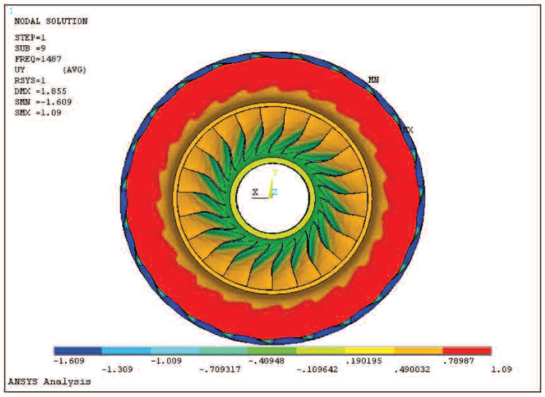

Figure 45. Zero Nodal Diameters Mode with Scallop Shaped Displacement Pattern for Modified Design.

The study of the natural mode shapes points toward two possible types of failures:

- Scalloped shaped failures in blades, and
- Scalloped shaped failures in a cover and/or disc.

The failure in blades can be attributed to tangential modes since blades vibrate primarily in the tangential direction. The scalloped shaped cover failure can be attributed to axial modes in which the primary displacement is in the direction of the axis of the machine.

The proven concept and the method of interference diagram that have been used successfully to design a bladed disc in a steam turbine and other types of turbomachinery can also be used for assessing the reliability of an impeller.

ACKNOWLEDGEMENTS

The authors express thanks to the management of GE Oil & Gas CONMEC for their support. The authors would also like to thank Michael Drosjack for his valuable suggestions.

REFERENCES

Bloch, H. P., 1996, *A Practical Guide to Steam Turbine Technology*, New York, New York: McGraw-Hill.

Ewins, D. J., 1970, "A Study of Resonance Coincidence in Bladed Discs," *Journal of Mechanical Engineering Science*, *12*, (5).

Ewins, D. J., 1973, "Vibrational Characteristics of Bladed Disk Assemblies," *Journal of Mechanical Engineering Science*, *15*, (3), pp. 165-185.

Jones, D. I. G. and Muszynska, A., 1983, "A Discrete Model of Multiple Blade System with Interblade Slip," Vibrations of Bladed Disk Assemblies, ASME, The Ninth Biennial Conference on Mechanical Vibration and Noise, Dearborn, Michigan, pp. 137-146.

Muszynska, A. and Jones, D. I. G., 1981, "A Parametric Study of Dynamic Response of a Discrete Model of Turbomachinery Bladed Disk," Proceedings of Eighth Biennial ASME Design Engineering Conference, ASME Paper 81-DET-137.

Nelson, W. E., 1979, "Maintenance Techniques for Turbomachinery," *Proceedings of the Eighth Turbomachinery Symposium*, Turbomachinery Laboratory, Texas A&M University, College Station, Texas, pp. 11-20.

Singh, M. P. and Schiffer, D. M., 1982, "Vibrational Characteristics of Packeted Bladed Discs," ASME Paper No. 82-DET-137.

Singh, M. P. and Vargo, J. J., 1989, "Reliability Evaluation of Shrouded Blading Using the SAFE Interference Diagram," *Journal of Engineering for Gas Turbine and Power*, *111*, pp. 601-609.

Singh, M. P., Vargo, J. J., Schiffer, D. M., and Dello, J. D., 1988, "Safe Diagram—A Design Reliability Tool for Turbine Blading," *Proceedings of the Seventeenth Turbomachinery Symposium*, Turbomachinery Laboratory, Texas A&M University, College Station, Texas, pp. 93-101.

Wang, Q., Bartos, J. C., and Houston, R. A., 1999, "Methodology of Open Bladed Impeller Resonance Identification," *Proceedings of the Twenty-Eighth Turbomachinery Symposium*, Turbomachinery Laboratory, Texas A&M University, College Station, Texas, pp. 61-68.